Progress In Electromagnetics Research B, Vol. 56, 137–160, 2013

DESIGN AND ANALYSIS OF MULTI-BAND FILTERS USING SLOT LOADED STEPPED IMPEDANCE RESONATORS

Rajas Khokle[1,*], Raj Kumar[2], Raghupatruni V.S.R. Krishna[1], and Nagendra Kushwaha[1]

[1]DIAT, Deemed University, Pune 411025, India

[2]ARDE, Pune 411021, India

Abstract—Two multi-band filters operating in the 1–10 GHz range are designed, analytically studied and experimentally verified. The filters are developed by making modifications to a series capacitively coupled, microstrip line filter. The middle section of the microstrip line is widened and rectangular slots are etched on it. Widening increases the effective dielectric constant which helps in miniaturization of the circuit. On the other hand, the rectangular slot cause various longitudinal, transverse and slot mode resonances to be excited resulting in multi-band operation. An extensive parametric analysis with respect to the physical parameters of the filter leading to the development of a semi-empirical model is presented. The model can be used to predict the resonant frequencies with sufficient accuracy for a given geometrical structure. The model also predicts the limit of miniaturization achievable with the presented design. The proposed filters besides being compact have good out of band rejection and are easy to design and fabricate without the need of additional matching circuits.

1. INTRODUCTION

The compact and high-performance microwave multi-band band-pass filters are playing an important role in the modern communication systems. The demand of such multi-band filters is continuously increasing in various wireless applications ranging from communication to sensor networks. Traditionally, a multi-band filter is synthesized by using the combination of two or more single-band filters [1]. A

Received 13 September 2013, Accepted 21 October 2013, Scheduled 25 October 2013

* Corresponding author: Rajas Khokle (rajask.ghr@gmail.com).

direct consequence of this approach, however, is increase in the size of filter. Apart from this, many designs require additional matching circuits which increase the complexity of the system [2]. Recently, some methods are investigated in theory as well as experiment to accommodate the multiple bands in a single filter. Guo et al. [3] designed dual-band filter in LTCC while Chang et al. [4] developed the hairpin dual-band filter and Hsieh and Chang [5] designed four cascaded open-loop ring resonators in microstrip band pass filter. The patch filter attracts lots of interests because of its simple and planar structure which is easy to fabricate by conventional PCB designing methods. These multi-band filters are composed of one or more dual-band patch resonators often in the form of square, rectangular, triangular, circular, or other modified shapes as in [6, 7]. More recently, the multi-band filters have also been realized utilizing the stepped impedance resonator concept [8–12].

A multiband filter can be designed by exploiting a basic property that a structure can resonate at all those frequencies for which its physical dimension will be an integral multiple of the wavelength associated with those particular frequencies. In this paper, a capacitively coupled series microstrip line resonator design is modified by first widening the middle section of microstrip line followed by etching of multiple rectangular slots on this microstrip line. Widening of microstrip line accomplishes three purposes namely increase in effective relative dielectric constant leading to miniaturization, decrease in the aspect ratio and provision of space for etching slots to tune the filter to various frequencies.

A detail study of effect of widening the central microstrip section is followed by an introduction of rectangular slot on this microstrip patch. It is found that the variation in slot's geometry modulates the resonances of the microstrip line in a periodic fashion. An extensive parametric study using an electromagnetic full wave analysis simulation tool Ansoft HFSS (High Frequency Structure Simulator) is done methodically. The analysis of the results is carried out by curve fitting the data obtained by full wave simulations of the various geometrical configurations of slot in filter. For curve fitting, MATLAB curve fitting tool has been extensively used with the customized modelling expressions. The modelling expressions are chosen based upon the careful observation of the current distribution on the filter for different configurations, as well as by taking into consideration the phenomena generating the observed response. Based on these studies semi-empirical formulations are generated for predicting the different resonant frequencies. Finally, for demonstration of the design methodology, two different filters are designed, fabricated and

tested. The calculated, simulated and experimental results are in close agreement with each other validating the analysis and design methodology presented in the paper. Finally, the conclusion is made in fifth section.

2. EVOLUTION OF A MULTIBAND FILTER

2.1. Design of a Capacitively Coupled Series Resonator and Effect of the Resonator Width

The design starts with the choice of high relative dielectric constant (ε_r) material. High dielectric constant is preferred for two reasons namely, miniaturization of filter and the fact that the fields are tightly bound in high ε_r material and so the filter does not radiate. Considering these factors, Rogers RT/Duroid 6010.5 substrate having $\varepsilon_r = 10.5$ and thickness 1.25 mm is used to design and fabricate the filters. A capacitively coupled series resonator as shown in Figure 1(a) acts as a resonant structure which can be used as a first order narrowband bandpass filter [13]. In order to match a 50 Ω SMA connector to a microstrip line, its width is calculated as 1 mm using the curve fit approximations to rigorous quasi static solutions given in [13]. First resonance for such a line would occur at $L = \lambda/2$, where L is the length of the middle section of microstrip line. Corresponding frequency can be calculated using Equation (1).

$$f = \frac{C}{\sqrt{\varepsilon}_{reff}\lambda} \tag{1}$$

However, such a narrow microstrip line would exhibit dispersion which means effective dielectric constant would be a function of frequency itself. Such a frequency dependant expression for effective dielectric

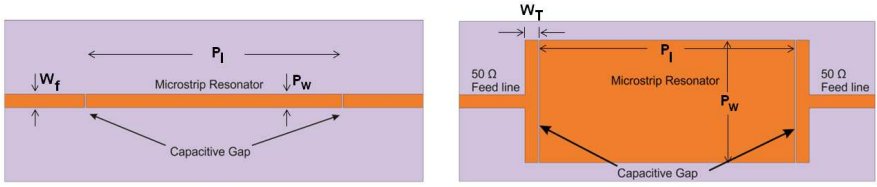

Figure 1. (a) Bandpass filter using the capacitively coupled narrow microstrip series resonator. (b) Bandpass filter using the capacitively coupled wide microstrip series resonator.

constant is first given by Getsinger [14], reproduced in Equation (2).

$$\varepsilon_{reff}(f) = \varepsilon_r - \frac{\varepsilon_r - \varepsilon_{reff}(0)}{1 + P(f)} \tag{2}$$

Here, $\varepsilon_{reff}(0)$ is the static effective permittivity at DC which can be calculated by using Equations (3a) and (3b)

$$\varepsilon_{reff}(0) = \begin{cases} \frac{\varepsilon_r+1}{2}\left[1-\frac{1}{2H}\left(\frac{\varepsilon_r-1}{\varepsilon_r+1}\right)\left(\ln\frac{\pi}{2}+\frac{1}{\varepsilon_r}\ln\frac{4}{\pi}\right)\right]^{-2}, & w/h < 1.3 \\ \varepsilon_{reff} = \frac{\varepsilon_r+1}{2} + \frac{\varepsilon_r-1}{2}\left(1+\frac{10h}{w}\right)^{(-0.555)}, & w/h > 1.3 \end{cases} \tag{3a}$$

$$H = \ln\left(4h/w + \sqrt{16(h/w)^2 + 2}\right) \tag{3b}$$

An accurate closed form expression for filling factor or frequency dependant term $P(f)$ in terms of the design parameters is given by Kirschning & Jansen (KJ Model) [15]. Using these expressions, it is found that for 1 mm width of the microstrip line, the value of ε_{reff} varies from 8 to 10.2 as frequency changes from 1 GHz to 10 GHz. As the width of microstrip line increases this variation decreases and the effective dielectric constant approaches to ε_r. For example, the microstrip line of width 9 mm ε_{reff} varies just from 10 to 10.4 for 1 GHz $< f <$ 10 GHz. Thus the design becomes relatively insensitive to the changes in relative dielectric constant offered by microstrip line. This makes initial design calculations easier as $\varepsilon_{reff} \approx \varepsilon_r$. Also as the width of the microstrip line increases the capacitance also increases and consequently the frequency of operation also decreases. This phenomenon allows us to design a filter with a smaller aspect ratio (length/width). Another advantage in increasing the width of the microstrip resonator is decrease in the Q factor, which translates into increase in bandwidth.

Considering these factors, the width of the central microstrip resonator is increased. The length of the central microstrip resonator patch is chosen as 19.2 mm so as to make it resonate at 2.4 GHz. The lengths of the 50 Ω lines which are connected to SMA connectors have no effect on resonances so their length is adjusted to 5 mm so as to facilitate the soldering of SMA connectors to the filter. A step in 50 Ω line having width equal to that of the microstrip resonator is introduced on either side of the resonator section creating a T shape section. This ensures maximum coupling of the electromagnetic energy from ports to the central microstrip section. Changing the width of T section (W_{T}) will effectively increase the resonant length of middle microstrip resonator which in turn will lower the operating frequency. From circuit point of view, increasing the width of T section increases the capacitance which lowers the resonant frequencies. While this

will not affect the lower frequencies, it can appreciably affect the higher frequencies. It can be noted that the effect will be only on the longitudinal modes, i.e., the resonances occurring along the length of the microstrip resonator. For the orthogonal/transverse modes, the width of T section will not matter but it will depend on the length of T-section which is equal to the patch width. Considering this, the width of T section is kept to a nominal value of 1 mm. The structure of this filter is as shown in Figure 1(b). The corresponding dimensions of the two filters are given in Table 1, while its equivalent circuit can be represented as shown in Figure 2. Here C_{T} is parallel capacitance offered by the impedance step and C_g is series gap capacitance.

Table 1. Dimensions (in mm) of the filters shown in Figure 1.

Parameter	Narrow Microstrip Filter	Wide Microstrip Filter
Resonator Length (P_l)	19.2	19.2
Resonator Width (P_w)	1.0	9.2
Capacitive Gap (C_g)	0.1	0.1
Feed Line/T Section Width (W_f/W_{T})	1.0	1.0

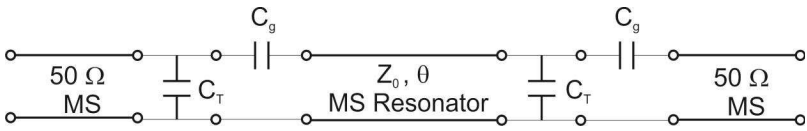

Figure 2. Equivalent circuit of the capacitively coupled wide microstrip series resonator filter.

2.2. Simulated Results for the Narrow and Wide Resonator Filters

Both the filters shown in Figure 1 are designed and simulated in Ansoft High Frequency Structure Simulator (HFSS). Figure 3 shows the graph of reflection co-efficient of both the filters. From this graph, it is seen that in 1 to 10 GHz frequency range, there are 3 resonances for the narrow microstrip filter shown in Figure 1(a), while for a wide microstrip filter shown in Figure 1(b), there are 4 resonances. A comparison of the resonant frequencies and their corresponding 3 dB bandwidths is given in Table 2. It can be seen from this data that the

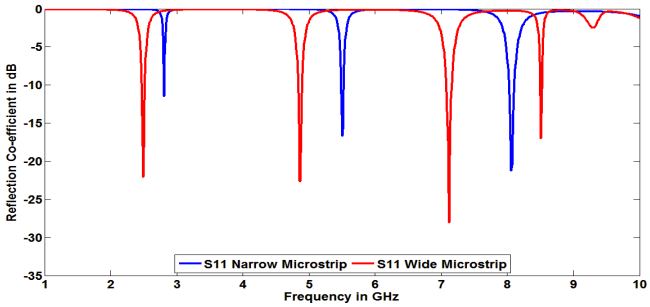

Figure 3. Comparison of the reflection coefficient of the narrow and wide microstrip capacitively coupled series resonator.

Table 2. Resonant frequencies and 3 dB bandwidths (in GHz) of the filters shown in Figure 1.

Parameters	F1	BW1	F2	BW2	F3	BW3	F4	BW4
Narrow Microstrip Filter	2.81	0.033	5.50	0.10	8.06	0.24	-	-
Wide Microstrip Filter	2.50	0.12	4.87	0.16	7.12	0.24	8.51	0.08

increase in the width decreases all the resonant frequencies along with an increase in bandwidth as expected and explained above.

2.3. Design Expressions and Calculated Results for the Narrow and Wide Resonator Filters

The current distribution at various resonant frequencies for the wide resonator filter is plotted in Figure 4. The current distribution clearly shows that the first three resonances are due to the excitation of the longitudinal modes whereas the fourth resonance is due to the excitation of the orthogonal/transverse mode along the width of the microstrip line.

From the current distribution shown in Figure 4, the generalized equation for the jth resonant wavelength of longitudinal mode can be given by Equation (4) where 'P_l' is the length of the patch.

$$\lambda_j = \frac{2P_l}{j} \tag{4}$$

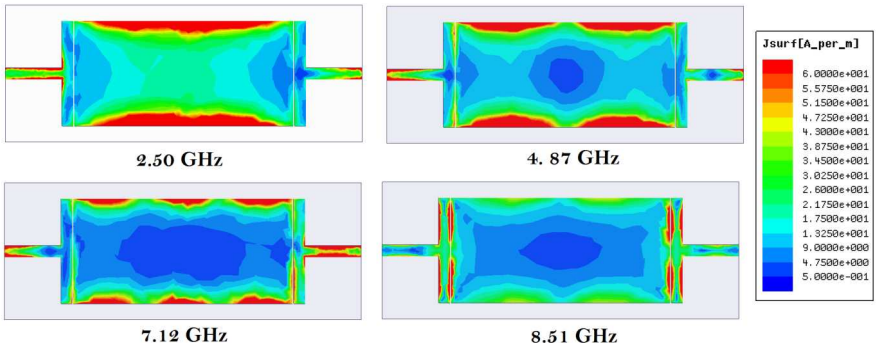

Figure 4. Current distribution of wide microstrip resonator filter at resonant frequencies.

For orthogonal/transverse modes, the kth resonance can be given by Equation (5) where 'P_{weff}' is the width of the patch. As fourth resonance is due to the transverse mode, Equation (5) is used. For this mode the patch acts like an open end whose width equal to the length of the patch. This open end offers extra capacitance which can be transformed in equivalent length extension (Δy). The effective width of the microstrip patch resonator is thus given by Equation (6). For $l/h < 3$, extension in length can be calculated using relations given by Garg & Bahl in [16], reproduced in Equation (7). For the wider microstrip line more accurate expressions are reported by Kirschning, Jansen & Koster (KJK model) in [17] by curve fitting the data obtained using hybrid full wave analysis. The expressions are reproduced in Equations (8) and (9a) to (9e). In the formulation given below, it has to be noted that the value of 'W' should be taken equal to P_l.

$$\lambda_k = \frac{P_{weff}}{k} \tag{5}$$

$$P_{weff} = P_w + 2\,(\Delta y) \tag{6}$$

$$\frac{\Delta y_{GB}}{h} = 0.412\frac{(\varepsilon_{reff} + 0.3)\left(\frac{W}{h} + 0.264\right)}{(\varepsilon_{reff} - 0.258)\left(\frac{W}{h} + 0.8\right)} \tag{7}$$

$$\frac{\Delta y_{KJK}}{h} = \frac{\xi_1\xi_3\xi_5}{\xi_4} \tag{8}$$

$$\xi_1 = 0.434907\frac{\varepsilon_{reff}^{0.81} + 0.26(W/h)^{0.8544} + 0.236}{\varepsilon_{reff}^{0.81} - 0.189(W/h)^{0.8544} + 0.87} \tag{9a}$$

$$\xi_2 = 1 + \frac{(W/h)^{0.371}}{2.358\varepsilon_r + 1} \tag{9b}$$

$$\xi_3 = 1 + \frac{0.5274 \arctan\left[0.084(W/h)^{1.9413/\xi_2}\right]}{\varepsilon_{reff}^{0.9236}} \tag{9c}$$

$$\xi_4 = 1 + 0.0377 \arctan\left[0.067(W/h)^{1.456}\right] \cdot \{6 - 5\exp\left[0.0361(1-\varepsilon_r)\right]\} \tag{9d}$$

$$\xi_5 = 1 - 0.218\exp\left(-7.5W/h\right) \tag{9e}$$

Using equations from (1) to (9) the resonant frequencies for the geometries shown in Figures 1(a) and 1(b) are calculated. The calculated and simulated frequencies and the % deviation are given in Table 3 below.

Table 3. Comparison of the calculated and simulated resonant frequencies for narrow and wide microstrip coupled resonator filters.

Frequency	f_1 (GHz)	f_2 (GHz)	f_3 (GHz)	f_4 (GHz)	
				(GB)	(KJK)
Calculated	2.41	4.82	7.23	9.03	8.41
Narrow Microstrip (HFSS)	2.81	5.5	8.06	-	-
% Deviation	13.53%	12.3%	10.29%	-	-
Wide Microstrip (HFSS)	2.50	4.87	7.12	8.51	8.51
% Deviation	3.6%	1.03%	1.54%	6.12%	0.69%

From Table 3, it can be seen that for a narrow microstrip line, the maximum % deviation is about 13.5% for the first resonant frequency. This deviation is because of not considering the effect of series capacitance offered by the gap in the microstrip sections. Capacitance in series decreases overall capacitance and so resonant frequency increases. In order to evaluate such a capacitance closed form expressions given in [7] can be used. However, the reported accuracy of such expression is within 7%. With increasing frequency the capacitance decreases and so there is a reduction in frequency and consequently the discrepancy between the calculated and simulated results decreases with increasing frequency.

For a wide central microstrip section, an impedance step has to be introduced in microstrip line for efficient electromagnetic coupling. This impedance step introduces capacitance C_{T} in parallel while the gap capacitance C_g is in series. The capacitance in series tends to decrease the total capacitance while that in parallel increases the total capacitance. So in a way, the increased width of the microstrip resonator compensates to some extent for the capacitance offered by

the gap. As a consequence the observed frequency is nearer to the calculated frequency and so the % deviation is less.

For the fourth resonant frequency, it can be seen right away that the KJK model predicts the resonant frequency with very high accuracy, the deviation being as small as 0.69% as compared to GB model with error of about 6.12%. This is expected since the validity of the GB model is for $l/h < 3$ which is violated as $l/h = 7.36$ for microstrip width of 9.2 mm.

2.4. Parametric Study for the Resonator Width

Next, a small parametric study is done by gradually increasing the width of the microstrip line. Figure 5 shows the change in resonant frequency with increasing microstrip width. It can be seen that as the microstrip width increases, the rate of change in frequency reduces, i.e., it shows saturation behaviour. It implies that increase in width beyond saturation will not change the longitudinal resonances. However, as explained above, an orthogonal mode is also excited along the width of the microstrip line. Increasing the width, therefore, will decrease the resonant frequency of this transverse mode in accordance with Equation (5). Also, from the figure it seems that higher resonances are more affected by the change in width of the microstrip resonator.

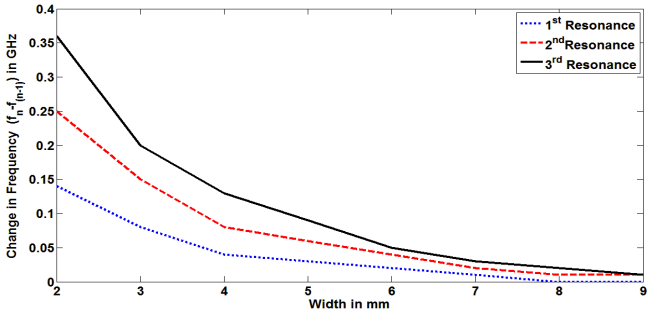

Figure 5. Effect of width of the microstrip resonator on the change in resonant frequencies.

However, for better interpretation of the effect of change in width on the higher resonances, the resonant frequencies for different widths are normalized with respect to the corresponding resonant frequencies of the narrow microstrip line (width = 1 mm). Figure 6 shows the plot of width of microstrip line versus a normalized frequency (f/f_0) for all the three resonances. Here, it can be observed that for all the resonances the % change in frequency for given width is same.

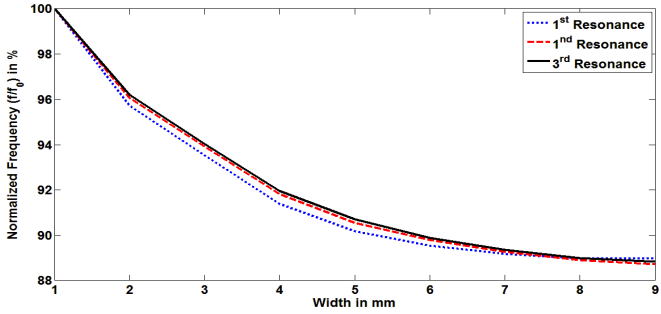

Figure 6. Normalized resonant frequencies versus width of microstrip resonator.

Moreover, it also reflects saturation behaviour. It seems that all the curves asymptotically reach to the maximum change of 12% as the width goes on increasing.

3. WIDE RESONATOR FILTER WITH RECTANGULAR SLOTS

3.1. Necessity of Slot and Its Effect on the Various Resonances

From the above studies, it is seen that increasing the width of microstrip resonator can reduce the frequency of operation, decrease the aspect ratio and increase the bandwidth. However designer does not have much control over the resonant frequencies since all the frequencies are affected by same percentage as seen from Figure 6. Also, reduction in frequency shows saturation behaviour and the maximum reduction possible is around 12%. In order to have control on the resonant frequencies and for further reduction in operating frequency, i.e., for further miniaturization, rectangular slots are etched on the microstrip resonator patch.

Once the width of the microstrip resonator is fixed, then for obtaining further change in resonant frequencies it is necessary to perturb the current on the microstrip resonator. From the current distribution shown in Figure 4, it can be seen that the current density is minimum in the center while it is maximum along the length of the microstrip resonator patch. Consequently, it can be deduced that etching the slot in the center of the patch will not affect resonant frequencies much while if the dimensions of slot are increased to disturb the current distribution along the edges of the patch, the resonant

frequencies will change.

In order to verify this premise, a narrow slot of length 2 mm (S_l) is etched at the centre of the microstrip resonator of Figure 1(b). Its width (S_w) is gradually varied from 1 mm to 9 mm and the effect on resonances is observed. A plot of effect of increasing the width of slot on the normalized resonant frequencies is given in Figure 7. Here the resonant frequencies of narrow microstrip coupled line filter are used for normalization of first three frequencies whereas for fourth resonance the fourth resonant frequency of wide microstrip coupled line filter is used.

Comparing Figure 6 and Figure 7, it can be readily observed that inclusion of a slot in the circuit has completely altered the frequency

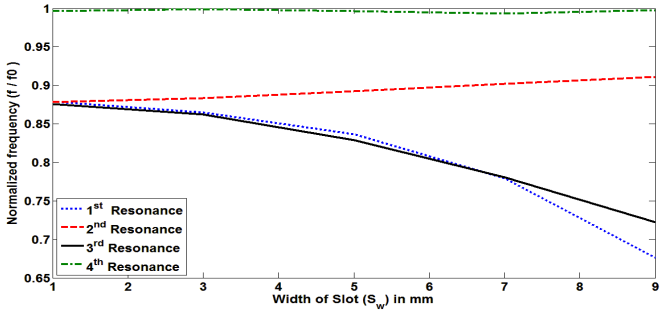

Figure 7. Effect of increasing slot width on the normalized resonant frequencies (f/f_0).

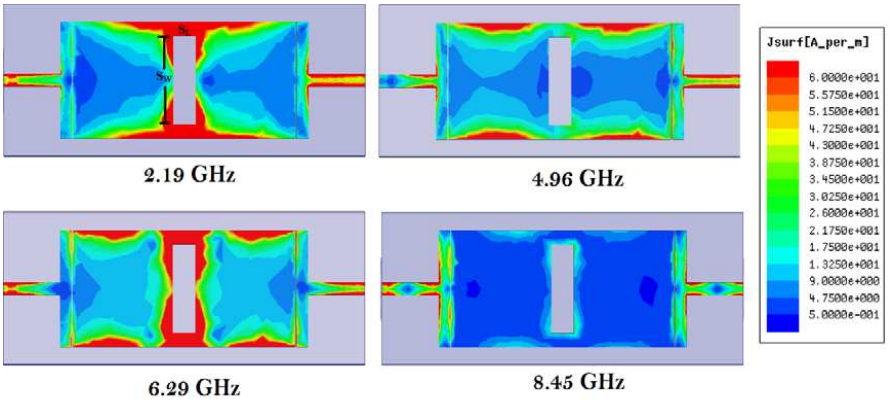

Figure 8. Current distributions at resonant frequencies for $S_w = 7$ mm.

response of the circuit along with further miniaturization in circuit. It is seen that for smaller widths there is no appreciable change in resonant frequencies but as the width increases f_1 & f_3 decrease, f_2 increases and f_4 remains fairly constant. In essence, the odd longitudinal frequencies decrease while even longitudinal frequencies increase and the transverse modes do not change. Also, the change in frequency is more for odd longitudinal mode than the even longitudinal mode. This behaviour can be explained by the help of current distribution, plotted for $S_w = 7\,\text{mm}$, in Figure 8.

From the current distribution at fourth resonance, it can be readily seen that since the slot length is small, it does not affect the current distribution along the width of the patch. Consequently, there is almost no change in the fourth frequency with increasing width of the slot which is due to transverse mode excitation.

Now for the second frequency, it is observed that there is a current minimum at the middle of the length. Since the slot offers high impedance at the centre the current minima is shifted away from the centre and so the path length for current decreases. Thus, the even longitudinal frequencies will shift towards higher end with increase in the length of the slot. In this case, since the length of the slot is same and width is changed, the change in the even longitudinal frequency is not expected. However, as the width of the slot increases, the fields tend to leak away more thereby reducing the effective dielectric constant. This in effect increases the resonant frequency slightly as is evident from the graph.

Next, it can be observed that for odd frequencies, the current maximum is around the center of the length of the microstrip resonator. Etching the slot in this region would increase the path length for the current and so the resonant frequency decreases. Consequently, greater the width of the slot more is the frequency shift. A general expression for the odd frequencies for the structures having narrow slots ($S_l < \lambda/10$), can be given by Equation (10).

$$\lambda_{2j+1} = \frac{2(P_l + S_w/2)}{2j+1}, \quad \text{For } j = 0, 1, 2, 3 \ldots \tag{10}$$

For determining frequency using Equations (1) & (10), $\varepsilon_{reff} \approx \varepsilon_r$ can be used as long as the slot length is small. It is therefore evident that the minimum frequency achievable by such a configuration is for $j = 0$ and when $S_w \approx P_w$ and $S_l \approx 0$. For the current circuit, this is equal to the lowest frequency of operation of 1.945 GHz or 30.93% lower with respect to the coupled narrow microstrip filter. However, if we allow for increase in S_l, i.e., a wide slot is etched it can be reasoned that, the fields will no longer be confined between patch and ground, which will decrease the effective dielectric constant and so increase

the operating frequency. However since path length will increase the resonant frequency will tend to decrease.

3.2. Parametric Study for the Slot Width and Generalized Expressions for Resonance Frequencies and Maximum Miniaturization Possible

To study the complex behaviour & in order to get an insight into the behaviour of the filter for various lengths and width of slots, an extensive parametric analysis by simultaneous variation of slot length (S_L) and slot width (S_W) is done and its effect on the first, second and third resonance is plotted in Figures 9, 10 and 11 respectively. The analysis of the results is done by curve fitting the data obtained by full wave simulations of the various configurations of filter.

Here, all the frequencies (f) are normalized with respect to the

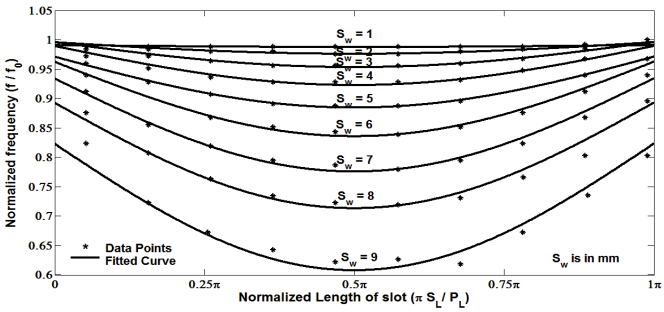

Figure 9. Effect of variation in length and width of slot on first resonant frequency.

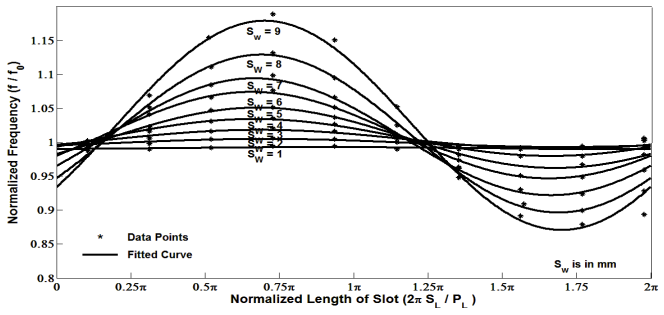

Figure 10. Effect of variation in length and width of slot on second resonant frequency.

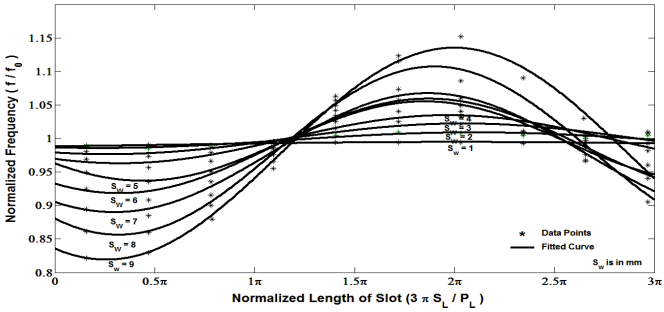

Figure 11. Effect of variation in length and width of slot on third resonant frequency.

resonant frequencies of the wide microstrip filter without slot (f_0). It is seen that for the first resonance the electrical length of the patch equals $\lambda/2$ or π degrees while for second and third resonance the length of patch equals 2π and 3π. For first resonance, it can be seen that the resonant frequency first decreases as the slot length increases from 0 to $\pi/2$ and again increases as the slot length increases beyond $\pi/2$ or equivalently beyond $\lambda/4$. For a second resonance also, the frequency first increases, then decreases and increases again completing a full wave. A similar variation is exhibited by the third resonance with recurring increment and decrement of resonant frequencies. All these variation in resonances are distinctively following sinusoidal patterns. It can be inferred therefore, that the slots of various lengths modulate the resonant frequency of the structure periodically. Therefore, this variation can in general be represented by a Fourier series. A generalized expression for the normalized frequency in terms of normalized length of the slot can thus be given by Equation (11). This expression is written for nth resonant frequency with 'm' Fourier coefficients. The inclusion of Θ_n in the phase term accounts for the non-linearity introduced due to the frequency dependant behaviour of the various capacitances like C_g and C_T which tend to vary the phase of the current.

$$\left(\frac{f}{f_0}\right)_n = \psi_n + \sum_{n,m} \zeta_{n,m} \sin\left(\Theta_n \cdot n\pi \frac{S_L}{P_L}\right) + \sum_{n,m} \xi_{n,m} \cos\left(\Theta_n \cdot n\pi \frac{S_L}{P_L}\right) \quad (11)$$

A goodness of fit analysis shows that for the first resonance, the cosine terms and higher sine terms in the Fourier series can be neglected. Also for $\Theta_1 = 1$ the model can predict the parametric data with sufficient accuracy. This follows from the fact that for lower frequencies various capacitances in series and parallel nullify each other's effect at

lower frequencies. It should be noted that the non-linear behaviour is most prominent at extreme configuration, i.e., for $S_L \approx P_L$ as capacitances are modified by the proximity of slot. In this case the minimum adjusted R^2 is about 0.9474 and maximum RMSE is 0.02. For maximum other points the adjusted R^2 is around 0.99 and RMSE is around 0.01. Thus simplified Equation (12) is sufficient to model the first resonance of the structure.

$$\left(\frac{f}{f_0}\right)_1 = \psi_1 + \zeta_{1,1} \sin\left(\pi \frac{S_L}{P_L}\right) \tag{12}$$

Now, the co-efficient ψ_1, $\zeta_{1,1}$ have to be evaluated such that they satisfy the limiting conditions given in Equation (13).

$$\left(\frac{f}{f_0}\right)_n = 1, \quad \text{for } S_W = 0 \quad \text{or } S_L = 0 \tag{13}$$

With these limiting conditions and taking into consideration the current distribution the Fourier coefficients can be modelled in terms of the physical parameters of the structure. In Equation (11), it can be observed that, ζ & ξ are the scaling functions for the sine and cosine terms and as evident from graph, they vary with the width of the slot. Thus, they can be modelled in the form of the equation $\zeta_{n,1} = A_n(S_W)^{B_n}$ & $\zeta_{n,1} = C_n(S_W)^{D_n}$. Similarly, ψ_1 accounts for the offset to the Fourier terms. As the width of the slot increases it will disturb more and more current and so it will tend to offset the resonant frequencies more and more. Now the current distribution along the width of the patch is exponential in nature decaying to zero at the centre and since the slot is etched symmetrically with respect to the width from center, the offset function for first resonance (in general odd resonances) should take the form of expression $\psi_1 = E_1 S_{L_{initial}}(1 - \exp(S_W/2)) + F_1$. The term $S_{L_{initial}}$ in the above expression refers to the minimum value of length of slot for which the parametric analysis is performed and its value is 1. For limiting condition, $S_{L_{initial}} = 0$ the offset function reduces to $\psi_1 = 0$ as required by Equation (13). Also, Equation (13) demands $F_1 = 1$. Consequently, by curve fitting the data obtained from the full wave analysis of the structure; ζ & ψ for first resonance can be given by Equations (14a) and (14b) respectively.

$$\psi_1 = 0.00196\,(1 - \exp\,(S_W/2)) + 1 \tag{14a}$$

$$\zeta_{1,1} = -0.02146(S_W)^{1.5} \tag{14b}$$

In order to evaluate the minimum frequency of operation for the circuit under investigation, the scaling function ζ should be at its minimum and sine function should be at its maximum owing to the negative sign in the expression of ζ. ζ can be minimum, if S_w is maximum

which is when $S_w \approx P_w$ and sine function can be at maximum for $S_L = 0.5P_L$. Also with the condition $S_w \approx P_w$ the value of the offset function ψ decreases which in turn reduces the resonant frequency. Thus putting these values of S_L & S_W in Equation (14) gives the minimum resonant frequency possible and consequently the maximum amount of miniaturization achievable. Upon such substitutions, the minimum value of the normalized frequency, in other words the limit of miniaturization; is given by Equation (15). With the current design having $P_w = 9.2\,\text{mm}$, the normalized frequency is 0.5854. Thus maximum miniaturization possible for this filter with respect to the wide microstrip filter is 41.45%.

$$\left(\frac{f}{f_0}\right)_{\min} = 1.04058 - 0.02784P_w - 0.002\exp\left(\frac{P_W}{2}\right) \tag{15}$$

For the second resonance, although the cos term cannot be neglected, the higher terms ($m > 1$) are still unwarranted. The parameter Θ_n can still be considered unity without the loss of much accuracy of the model while predicting the full wave analysis data. Consequently, expression for second resonance can be written as Equation (16).

$$\left(\frac{f}{f_0}\right)_2 = \psi_2 + \zeta_{2,1}\sin\left(2\pi\frac{S_L}{P_L}\right) + \xi_{2,1}\cos\left(2\pi\frac{S_L}{P_L}\right) \tag{16}$$

Also, for the second resonance (or in general even frequencies), it is the length of the slot which plays a crucial role in changing the frequency as explained previously. However increasing the width increases the effect of the length and again as the current distribution along the width is exponential and as initially the resonant frequency increases, the offset function should take the form of $\psi_2 = E_2 S_{L_{initial}} \exp(S_W/2) + F_2$, again with $F_2 = 1$. The corresponding values of Fourier coefficients ψ_2, $\zeta_{2,1}$ and $\xi_{2,1}$ are given by Equations 17(a), 17(b) & 17(c) respectively.

$$\psi_2 = 0.0002173\exp(S_W/2) + 1 \tag{17a}$$

$$\zeta_{2,1} = 0.001523S_W^2 \tag{17b}$$

$$\xi_{2,1} = -0.0003646S_W^{2.5} \tag{17c}$$

For the third resonance, the Θ_n cannot be neglected and considered as unity. Consequently, the model for curve fitting takes the form of Equation (18).

$$\left(\frac{f}{f_0}\right)_3 = \psi_3 + \zeta_{3,1}\sin\left(\Theta_3 \cdot 3\pi\frac{S_L}{P_L}\right) + \xi_{3,1}\cos\left(\Theta_3 \cdot 3\pi\frac{S_L}{P_L}\right) \tag{18}$$

Since Θ_n depends upon the capacitances due to the gap, impedance step and slot, all of which depend on patch and slot width; the

variation in Θ_n should be modelled by an expression having form $\Theta_3 = G_n(S_W/P_W)^{H_n} + K_n$ where G_n, H_n & K_n are coefficients of curve fitting. The corresponding values of the various coefficients of Equation (18) are given by Equations (19a), (19b), (19c) and (19d). Goodness of fit analysis shows the minimum adjusted R^2 is 0.9618 and RMSE is 0.0052 for this fit.

$$\psi_3 = 0.0006119(1 - \exp(S_W/2)) + 1 \tag{19a}$$

$$\zeta_{3,1} = -0.003115S_W^{1.45} \tag{19b}$$

$$\xi_{3,1} = -0.001151S_W^{2.17} \tag{19c}$$

$$\Theta_3 = -0.03354(S_W/P_W)^{-1} + 0.6816 \tag{19d}$$

Summarizing, the addition of slot of various lengths and widths can alter the frequency response of the filter. This change in frequency is sinusoidal in nature and can be represented by the Fourier series expansion. The slots of proper length and width etched on the patch are capable of tuning the individual frequencies. It is also observed that the effectiveness of the slot increases with its proximity to the edge of the patch.

4. CONFIGURATION OF THE PROPOSED BAND PASS FILTERS

Based on this study and analysis presented in the previous sections, two multiband filters as shown in Figure 12(a) and Figure 12(b) is designed. The dimensions corresponding to the labels shown in Figures 12(a) & 12(b) are given in Table 4.

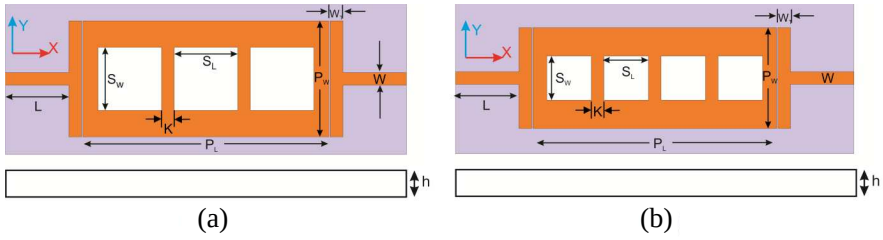

Figure 12. (a) Configuration of the proposed three slot band pass filter. (b) Configuration of the proposed four slot band pass filter.

Table 4. Optimized dimensions (in mm) of the proposed three and four slot band pass filter.

Parameters (mm)	P_L	P_W	L	W	K	S_L, S_W
3-slot filter	19.2	9.2	5	1.0	1.0	5.0, 5.0
4-slot filter	19.2	7.0	5	1.0	1.0	3.5, 3.5

It is evident that the transverse mode is efficiently excited when the edge of the slot is nearer to the transverse dimension of the patch or in other words when slot length is near to the patch length. A slot itself is capable of resonating at frequencies for which its perimeter is integral multiple of the wavelength. However for the case of rectangular slot fed from smaller dimension the impedance matching is very poor and thus it may not excite the slot mode. In order to excite all three kinds of resonances namely three longitudinal modes, transverse mode and slot mode a split slot configuration is proposed. In first design a single slot is split into 3 equal symmetrically placed slots as shown in Figure 12(a).

In the second design Figure 12(b), a single large slot is split into four equal and symmetrically placed slots. Second design prominently demonstrates the use of splitting the slots in order to modify the transverse mode. The prediction of this resonance can be done by using equations for second longitudinal mode with the definitions length and width interchanged for both slot and patch. These results become more accurate with the use of KJK model for evaluating the length of the patch along transverse dimension. The slot mode resonance in this design has been shifted beyond 10 GHz by decreasing the size of the slot to 3.5 mm × 3.5 mm. Figure 13 shows the equivalent circuit with L_s and C_s being the inductance and capacitance offered by the slots etched on the microstrip resonator patch.

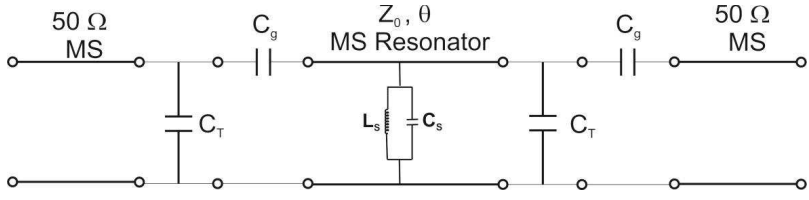

Figure 13. The equivalent circuit of the slot loaded series coupled microstripline filter.

5. EXPERIMENTAL RESULTS OF THE PROPOSED FILTERS

The proposed filters shown in Figures 3(a) and 3(b) are designed and fabricated with the optimized dimensions. The photographs of the fabricated three slot and four slot filters, are as shown in the Figure 14. These filters circuits were assembled and tested using in

Figure 14. Photograph of the fabricated prototypes of the 3-slot and 4-slot multiband band pass filters.

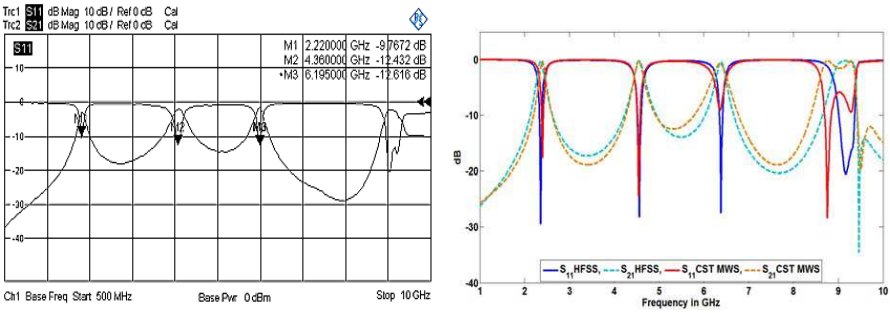

Measured Simulated

Figure 15. Measured and simulated results of 3-slot filter.

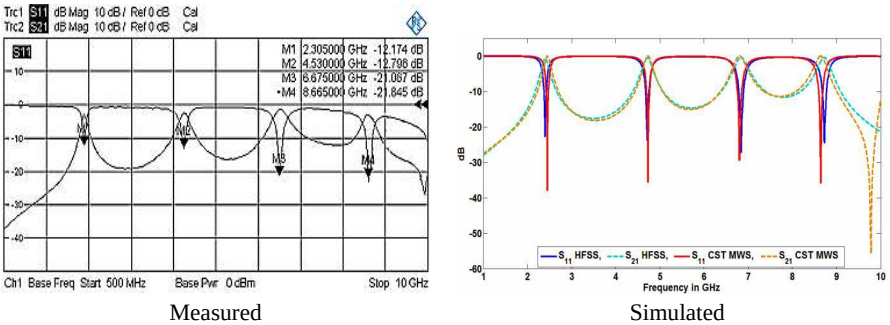

Measured Simulated

Figure 16. Measured and simulated results of 4-slot filter.

house R & S ZVA40 vector network analyser. The experimental and simulated results for the 3-slot filter and 4-slot filter are shown in Figure 15 and Figure 16 respectively. Table 5 shows the comparison of the calculated, simulated and observed resonant frequency of the two proposed filters. For the calculations of the first three frequencies, the empirical expressions developed in the previous section are used solutions are used. For transverse modes, KJK models are used. While the longitudinal resonances can be calculated based upon the total length and width occupied by all the slots, the slot resonance has be calculated based on the perimeter of individual slot. Also, for slot modes ε_{reff} is calculated according to the KJ dispersion model. It can be seen that the calculated simulated and observed resonances are in closed agreement with each other, thereby validating the analysis done so far and the design methodology presented.

Table 5. Comparison of the calculated, simulated and experimental resonant frequencies (in GHz) of 3-slot and 4-slot multiband bandpass filter.

Parameter	f_1 (GHz)	f_2 (GHz)	f_3 (GHz)	f_4 (GHz)	f_{slot} (GHz)
3-slot Filter (Calculated)	2.346	4.7	6.77	8.94	9.29
3-slot Filter (Simulated)	2.32	4.48	6.32	9.17	9.35
3-slot Filter (Measured)	2.23	4.39	6.21	9.07	9.26
4-slot Filter (Calculated)	2.35	4.785	7.04	8.68	-
4-slot Filter (Simulated)	2.40	4.71	6.84	8.73	-
4-slot Filter (Measured)	2.305	4.530	6.675	8.665	-

In order to complete the analysis Table 6 gives the comparison of simulated and measured center frequency and 3 dB bandwidths for the 3-slot and 4-slot multiband filters. F_c is the center frequency and F_L & F_H are lower and higher 3 dB cut-off frequencies which define bandwidth (BW). It can be seen that the simulated results are in close agreement with the experimental results.

In order to verify the transmission modes, a current distribution plot for a 3-slot and 4-slot filter at resonant frequencies is plotted

Table 6. Measured and simulated results of 3-slot & 4-slot filters.

3-slot filter				4-slot Filter			
Measured Results				Measured Results			
F_c GHz	F_L GHz	F_H GHz	BW GHz	F_c GHz	F_L GHz	F_H GHz	BW GHz
2.23	2.13	2.31	0.18	2.305	2.21	2.35	0.14
4.39	4.24	4.54	0.30	4.530	4.38	4.62	0.24
6.21	6.08	6.29	0.21	6.675	6.51	6.86	0.35
9.07	8.91	9.39	0.48	8.665	8.51	8.79	0.28
Simulated Results				Simulated Results			
F_c GHz	F_L GHz	F_H GHz	BW GHz	F_c GHz	F_L GHz	F_H GHz	BW GHz
2.36	2.28	2.44	0.16	2.40	2.32	2.48	0.16
4.56	4.46	4.68	0.22	4.71	4.60	4.82	0.22
6.39	6.29	6.49	0.20	6.84	6.69	6.99	0.30
9.17	8.89	9.4	0.51	8.73	8.58	8.86	0.28

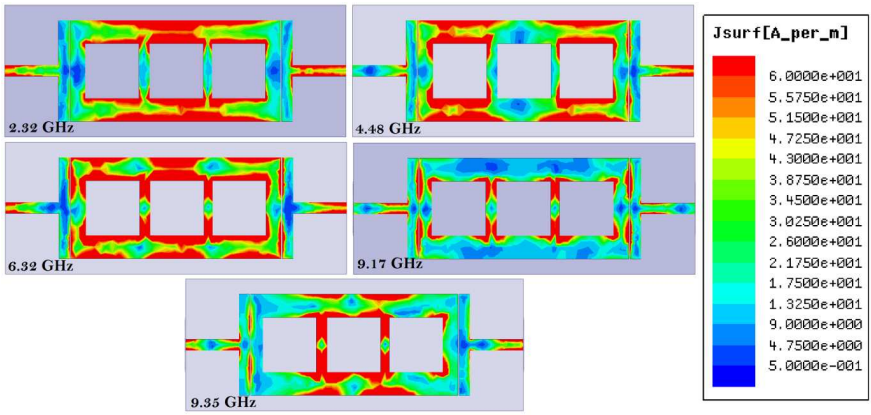

Figure 17. Current distribution of three slot filter at different resonant frequencies.

in Figure 17 & Figure 18 respectively. Figure 17 clearly shows that first three resonances are the longitudinal modes whereas the fourth resonance is transverse mode. At 9.35 GHz, it can be seen that the slot resonates predominantly at its second resonance. Similarly, Figure 18

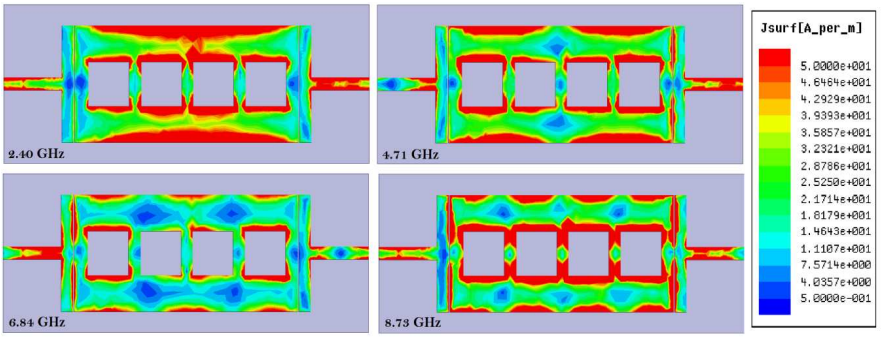

Figure 18. Current distribution of three slot filter at different resonant frequencies.

the current distribution clearly shows that first three are longitudinal resonances while fourth one is transverse excitation assisted by the 4th slot. The current distribution also suggests that the fourth resonance is modified by the presence of slot in a manner similar to the modification of second longitudinal resonance by the presence of slot. Consequently, same expressions can be used to calculate the resonant frequency.

6. CONCLUSIONS

A multiband bandpass filter design has been presented in this paper. A capacitively coupled series microstrip line resonator is modified by first widening the middle section of the microstrip line followed by etching of multiple rectangular slots on this section. A detail analysis of the effect of etching the slot on the central microstrip section has led to the development of a semi-empirical model predicting the resonant frequencies of the filter. The limit of miniaturization for such a filter is also evaluated by this model. Based on this model, a 3-slot filter has been designed and experimentally validated to give a quad band response. The first three resonances obtained are longitudinal resonances whereas the fourth is a wideband obtained by merging of the 1st transverse and the 2nd slot resonance. A 4-slot filter with quad band response is also designed and experimentally tested to verify the modulation effect of the slot on the longitudinal and transverse resonances. The designed filters have several advantages including compact size, multiband operation, sufficient out of band rejection, simpler design andease of fabrication and assembling. Furthermore, no additional matching circuits are required. The filters are expected to be useful in a host of wireless applications requiring multiband operation.

ACKNOWLEDGMENT

The authors would like to thank the Vice Chancellor of DIAT, Pune, India for all the support and encouragement. They would also like to thank the Ph.D. and M.Tech. Students of the Microwave and Millimetre wave Antenna Lab, DIAT for the fruitful discussions.

REFERENCES

1. Miyake, H., S. Kitazawa, T. Ishizaki, T. Yamada, and Y. Nagatomi, "A miniaturized monolithic dual band filter using ceramic lamination technique for dual mode portable telephones," *IEEE MTT-S International Microwave Symposium Digest*, Vol. 2, 789–792, 1997.
2. Kuo, J. T. and H. S. Cheng, "Design of quasi-elliptic function filters with a dual-passband response," *IEEE Microwave & Wireless Component Letters*, Vol. 14, No. 10, 472–474, 2004.
3. Guo, Y. X., L. C. Ong, M. Y. W. Chia, and B. Luo, "Dual-band band pass filter in LTCC," *IEEE MTT-S International Microwave Symposium Digest*, Jun. 2005.
4. Chang, S. F., Y. H. Jeng, and J. L. Chen, "Dual-band step-impedance bandpass filter for multimode wireless LANs," *Electronics Letters*, Vol. 40, No. 1, 38–39, 2004.
5. Hsieh, L. H. and K. Chang, "Compact size and low insertion loss Chebyshev-function bandpass filters using dual-mode patch resonators," *Electronics Letters*, Vol. 37, No. 17, 67–70, 2001.
6. Hong, J. S. and M. J. Lancaster, *Microstrip Filters for RF/Microwave Applications,* John Wiley, New York, 2001.
7. Gupta, K. C., R. Garg, I. J. Bahl, and P. Bhartia, *Microstrip Lines and Slotlines,* 2nd Edition, Artech House, Boston, 1996.
8. Yang, R.-Y., C.-Y. Hung, and J.-S. Lin, "Design and fabrication of a quad-band band pass filter using multi-layered SIR Structure," *Progress In Electromagnetics Research*, Vol. 114, 457–468, 2011.
9. Yang, C.-F., Y.-C. Chen, C.-Y. Kung, J.-J. Lin, and T.-P. Sun, "Design and fabrication of a compact quad-band band pass filter using two different parallel positioned resonators," *Progress In Electromagnetics Research*, Vol. 115, 159–172, 2011.
10. Lin, W.-J., C.-S. Chang, J.-Y. Li, D.-B. Lin, L.-S. Chen, and M.-P. Houng, "A new approach of dual band filters by stepped impedance simplified cascaded quadruplet resonators with slot coupling," *Progress In Electromagnetics Research Letters*, Vol. 9, 19–28, 2009.

11. Wei, F., Q. Huang, X. H. Wang, W.-T. Li, and X.-W. Shi, "Compact stepped impedance ring resonator for quad-band band pass filter," *Progress In Electromagnetics Research Letters*, Vol. 41, 105–112, 2013.
12. Ning, H., J. Wang, Q. Xiong, and L.-F. Mao, "Design of planar dual and triple narrow band band stop filters with inadvertently controlled stop bands and improved spurious response," *Progress In Electromagnetics Research*, Vol. 131, 259–274, 2012.
13. Pozar, D. M., *Microwave Engineering,* 4th Edition, John Wiley & Sons Inc., NJ, 2011.
14. Getsinger, W. J., "Microstrip dispersion model," *IEEE Transactions on Microwave Theory and Techniques*, Vol. 21, No. 1, 34–39, 1973.
15. Kirschning, M. and R.H. Jansen , "Accurate model for effective dielectric constant of microstrip with validity up to millimetre-wave frequencies," *Electronic Letters*, Vol.18, No. 6, 272–273, 1982.
16. Garg, R. and I. J. Bahl, "Microstrip discontinuities," *International Journal of Electronics*, Vol. 45, No. 1, 81–87, 1978.
17. Kirschning, M., R. H. Jansen, and N. H. K. Koster, "Accurate model for open end effect of microstrip lines," *Electronics Letters*, Vol. 17, No. 3, 123–125, 1981.